First-principles electronic transport calculations in finite elongated systems: A divide and conquer approach

Oded Hod,[a] Juan E. Peralta, and Gustavo E. Scuseria
Department of Chemistry, Rice University, Houston, Texas 77005

We present a *first-principles* method for the evaluation of the transmittance probability and the coherent conductance through *elongated* systems composed of a repeating molecular unit and terminated at both ends. Our method is based on a divide and conquer approach in which the Hamiltonian of the elongated system can be represented by a block tridiagonal matrix, and therefore can be readily inverted. This allows us to evaluate the transmittance and the conductance using first-principles electronic structure methods without explicitly performing calculations involving the entire system. A proof of concept model based on a *trans*-polyacetylene chain bridging two aluminum leads indicates that our divide and conquer approach is able to capture all the features appearing in the transmittance probability curves obtained by a full scale calculation. © *2006 American Institute of Physics.* [DOI: 10.1063/1.2349482]

I. INTRODUCTION

The theoretical evaluation of the electronic transport through molecular systems has been the focus of many studies in the past few decades. Since the original suggestion of Aviram and Ratner[1] to utilize a molecule for the fabrication of a nanoscale electronic device, the scientific community has paid attention to the study of small molecular candidates for future molecular electronic components.[2–11] When considering single molecule transport, one technologically promising and scientifically interesting branch of materials is one-dimensional elongated molecules. Systems such as carbon nanotubes,[12–20] graphene ribbons,[21,22] conducting polymers,[23–25] and biological molecules such as DNA (Refs. 26–29) exhibit high potential to serve as quantum wires and as electronic elements in future nanoscale electronic devices. Moreover, such molecules serve as model systems for the experimental and the theoretical study of the physical phenomena characterizing low-dimensional systems.

Due to the computational complexity of conductance calculations, many groups focus on very short and/or infinitely long periodic molecules. Several theoretical investigations have addressed the issue of finite extended systems using tight binding approximations.[30–36] A linear scaling approach[37] has been utilized to investigate the device-lead coupling effects on the conductance through carbon nanotubes with length shorter than 3 nm. Nevertheless, it is predicted that finite size effects may persist up to hundreds of nanometers.[31]

It is the purpose of the present study to introduce a *first-principles* theoretical approach for the evaluation of the transport properties of long molecules, which with current computational resources cannot be treated using "brute force" first-principles conductance calculations. We extend the work of Anantram and Govindan[30] to give a *first-principles* treatment of the conductance through finite extended molecules composed of a repeating unit and terminated at both ends. Similar ideas were employed in other studies utilizing the principal-layer method for the calculations of semi-infinite systems and surfaces.[38–43] Our method is based on a divide and conquer approach in which the elongated molecule is divided into a left part, a middle part, and a right part. The left (right) part interacts directly with the left (right) lead, while the middle part has no direct interaction with the leads. Computational efficiency is gained in both parts of the calculation, the electronic structure phase and the Green's function (GF) evaluation phase. On the electronic structure part, we assume that the middle part is composed of a repeating unit such that the Hamiltonian matrix of the elongated molecule in a localized basis set representation can be approximated as a block tridiagonal matrix with a replicated middle block. By representing this repeating block as the corresponding block of an infinite periodic system we replace the calculation of the electronic structure of the full finite elongated device by a calculation of the corresponding infinitely long periodic system which can be accomplished with much less computational effort. Using the sparsity of the Hamiltonian matrix of the full open system, we employ an efficient partial inversion algorithm to calculate only the relevant nonzero submatrices of the GF that contain all the information needed for the evaluation of the transport properties of the system.

We verify the validity of our assumptions using a simple model of a *trans*-polyacetylene (TPA) chain bridging two aluminum leads. Comparing the transmittance probability as calculated using our divide and conquer approach to that obtained by a full calculation of the elongated TPA system, we find that the divide and conquer approach is able to accurately capture all of the physical features appearing in the transmittance probability curve obtained using the full system. We quantify the accuracy of our approximation using a statistical cross-correlation analysis.

---

[a]Electronic mail: oded.hod@rice.edu

The rest of this paper is organized as follows. In Sec. II we present the divide and conquer computational approach. First, we give a brief overview of the general GF method for conductance calculations (Sec. II A), then we address the dimensionality scaling of such calculations for finite sized extended systems (Sec. II B), in Sec. II C we present the algorithm for the efficient calculation of the relevant blocks of the full GF matrices. Section II D is devoted to the description of the implementation using density functional theory calculations to obtain the input submatrices needed for the calculation. In Sec. III we show results for the TPA model system. A qualitative and quantitative assessment of the performance of our approximation is given therein. Finally, in Sec. IV we summarize and briefly discuss future directions.

II. COMPUTATIONAL METHOD

A. General formalism

In the current study, we are interested in calculating the conductance through a [lead|molecular-device|lead] geometry. For simplicity, we apply the Landauer formalism,[44,45] which relates the current and the conductance to the probability of an electron approaching the device from one lead to leave the device at the other lead. It should be mentioned that our method can be applied in conjunction with nonequilibrium Green's function formalism as well. At finite temperature and bias the current-voltage relation, within the Landauer framework, can be expressed in the following manner:[46]

$$I(V_b) = \frac{2e}{h} \int [f_L(E, \mu_L(V_b)) - f_R(E, \mu_R(V_b))] T(E) dE,$$

(1)

where I is the current, V_b is the bias voltage, e is the electron charge, h is Planck's constant, $T(E)$ is the transmittance probability, and E is the energy integration variable. The Fermi occupation functions of the left and the right leads are given by $f_{L/R}(E, \mu_{L/R}) = 1/[e^{\beta(E - \mu_{L/R})} + 1]$, where $\beta = 1/(k_B T)$, k_B is Boltzmann's constant, and T is the temperature. We assume that the bias voltage drops sharply at the two leads/device junctions[47] such that the chemical potentials of the leads have the form $\mu_L(V_b) = E_F^L - 0.5eV_b$ and $\mu_R(V_b) = E_F^R + 0.5eV_b$, E_F^L and E_F^R being the Fermi energies of the left and right leads, respectively. The differential conductance g is then given as the derivative of the calculated current with respect to the applied bias voltage,

$$g(V_b) = \frac{\partial I}{\partial V_b} = \frac{2e}{h} \int \frac{\partial [f_L(E, \mu_L(V_b)) - f_R(E, \mu_R(V_b))]}{\partial V_b} T(E) dE.$$

(2)

Here, we assume that the transmittance probability is bias independent. This approximation is valid only for low bias voltages where the electronic structure of the system is considered to be only slightly perturbed by the bias voltage.

In the above equations the main physical quantity needed to be evaluated is the transmittance probability, which is calculated using the following trace formula:[46,48,49]

$$T(E) = \text{Tr}[\Gamma_L(E) G_d^r(E) \Gamma_R(E) G_d^a(E)].$$

(3)

Here, $G_d^r(E)$ is the retarded Green's function (rGF) of the device, and $G_d^a(E) = [G_d^r(E)]^\dagger$ is the advanced Green's function of the device. $\Gamma_L(E)$ and $\Gamma_R(E)$ are the left and right broadening functions, respectively.

In a localized basis set representation, such as Gaussian- or Slater-type orbitals, the device's rGF is one block of the rGF matrix of the full system (leads+device). The latter is defined as

$$(\epsilon S - H) G^r(\epsilon) = I,$$

(4)

where $G^r(\epsilon)$ is the rGF matrix of the full system, H is the matrix representation of the Hamiltonian of the full system, S is the corresponding overlap matrix, $\epsilon = E + i\eta$, $\eta \to 0^+$, and I is the unit matrix of appropriate dimensions. It is convenient to formally divide the system into three subsystems, namely, the *left lead* (LL), the *device* (d), and the *right lead* (RL).

When doing so, Eq. (4) takes the following matrix form:

$$\begin{pmatrix} \epsilon S_{LL} - H_{LL} & \epsilon S_{LL,d} - V_{LL,d} & 0 \\ \epsilon S_{d,LL} - V_{d,LL} & \epsilon S_d - H_d & \epsilon S_{d,RL} - V_{d,RL} \\ 0 & \epsilon S_{RL,d} - V_{RL,d} & \epsilon S_{RL} - H_{RL} \end{pmatrix}$$
$$\times \begin{pmatrix} G_{LL}^r & G_{LL,d}^r & G_{LL,RL}^r \\ G_{d,LL}^r & G_d^r & G_{d,RL}^r \\ G_{RL,LL}^r & G_{RL,d}^r & G_{RL}^r \end{pmatrix} = \begin{pmatrix} I & 0 & 0 \\ 0 & I & 0 \\ 0 & 0 & I \end{pmatrix}.$$

(5)

Here S_{LL} and H_{LL} are the overlap and Hamiltonian matrices of the semi-infinite left lead, S_d and H_d are the overlap and Hamiltonian matrices of the device, S_{RL} and H_{RL} are the overlap and Hamiltonian matrices of the semi-infinite right lead, $S_{LL,d}$ and $V_{LL,d}$ are the overlap and coupling matrices between the left lead and the device, $S_{d,RL}$ and $V_{d,RL}$ are the overlap and coupling matrices between the device and the right lead,

$$S_{d,LL} = S_{LL,d}^\dagger, \quad V_{d,LL} = V_{LL,d}^\dagger, \quad S_{RL,d} = S_{d,RL}^\dagger, \quad V_{RL,d} = V_{d,RL}^\dagger,$$

and I is the identity matrix of the relevant size. The GF matrix is divided into nine corresponding blocks. In Eq. (5) it is explicitly assumed that the leads do not interact directly, by setting their coupling and overlap matrices to zero.
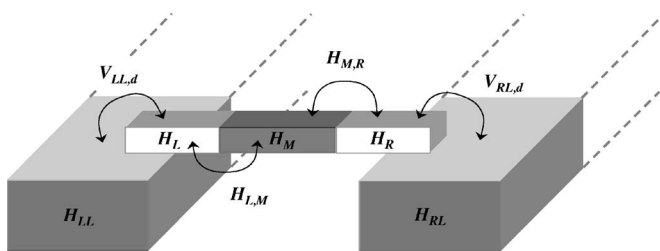
FIG. 1. A schematic representation of the division of the device into three parts: left (L), middle (M), and right (R). The left part of the device directly couples to the semi-infinite left lead (LL) while the right part of the device directly couples to the semi-infinite right lead (RL). There is no direct coupling between the middle part of the device and the leads.

Solving Eq. (5) for the middle column of G^r results in the following expression for the rGF of the device:

$$G_d^r(\epsilon) = [(G_d^{r0}(\epsilon))^{-1} - \Sigma_L^r(\epsilon) - \Sigma_R^r(\epsilon)]^{-1}. \qquad (6)$$

Here $G_d^{r0}(\epsilon) = [\epsilon S_d - H_d]^{-1}$ is the rGF of the bare device, and $\Sigma_{j=L/R}^r(\epsilon)$ is the retarded self-energy of lead j, which is given by the following expression:

$$\Sigma_{j=L/R}^r(\epsilon) = (\epsilon S_{d,jL} - V_{d,jL}) G_j^{r0}(\epsilon)(\epsilon S_{jL,d} - V_{jL,d}), \qquad (7)$$

where $G_j^{r0}(\epsilon)$ is the rGF of the isolated semi-infinite lead j. $G_j^{r0}(\epsilon)$ can be calculated using efficient iterative procedures.[39–41]

The broadening functions appearing in Eq. (3) can be written in terms of the leads self-energies in the following manner:[46,48,49]

$$\Gamma_{j=L/R}(\epsilon) = i[\Sigma_j^r(\epsilon) - \Sigma_j^a(\epsilon)], \qquad (8)$$

where i is the imaginary unit and $\Sigma_j^a(\epsilon) = [\Sigma_j^r(\epsilon)]^\dagger$.

B. Finite extended systems: Dimensionality scaling

At a first glance on the expression appearing in Eq. (3), it seems that the entire rGF matrix of the device, $G_d^r(\epsilon)$, needs to be calculated at each energy point in order to obtain the transmittance probability. For small molecules this is easily achieved; however, since our goal is the calculation of the conductance through finite but extended systems this can become a major obstacle. Nevertheless, if one carefully examines the equations, a remarkable simplification can be found to overcome this problem. This simplification is based on the fact that we are considering a localized basis set. In such a basis set, the range of the interactions between the leads and the device is relatively short such that we can further divide the *device* into three parts: the *left* part (L) of the device which directly couples to the left lead, the *right* part (R) of the device which directly couples to the right lead, and the *middle* part (M) of the device which couples only to its adjacent left and right counterparts. This division is shown schematically in Fig. 1. The device Hamiltonian can be written in matrix form as follows:

$$H_d = \begin{pmatrix} H_L & H_{L,M} & 0 \\ H_{M,L} & H_M & H_{M,R} \\ 0 & H_{R,M} & H_R \end{pmatrix}, \qquad (9)$$

where H_L is the left part Hamiltonian matrix, H_M is the middle part Hamiltonian matrix, H_R is the right part Hamiltonian matrix, $H_{L,M}$ is the coupling matrix between the left part and the middle part, $H_{M,R}$ is the coupling matrix between the middle part and the right part, and H_d is Hermitian such that $H_{M,L} = H_{L,M}^\dagger$ and $H_{R,M} = H_{M,R}^\dagger$. We assume that the left and right parts do not directly couple such that $H_{L,R} = H_{R,L}^\dagger = 0$. The corresponding overlap matrix, S_d, can be divided in a similar way.

As mentioned above, we assume that the left lead interacts only with the left part of the device. Since our basis set is localized, we can divide the semi-infinite periodic lead into blocks (often referred to as principal layers[39–41]) large enough such that only the block adjacent to the left part of the device couples with it. The lead-device coupling matrix, $V_{LL,d}$, can now be written in the following form:

$$V_{LL,d} = \begin{pmatrix} ** & 0 & 0 \\ 0 & 0 & 0 \\ 0 & 0 & 0 \\ \vdots & \vdots & \vdots \end{pmatrix}, \qquad (10)$$

where the three columns relate to the coupling of the different blocks of the lead with the left, middle, and right parts of the device, respectively, and only a single block (denoted by asterisks) in $V_{LL,d}$ is nonzero. The $S_{LL,d}$ matrix has the same form as in Eq. (10).

In the same manner one finds that the right lead-device coupling matrix has the form

$$V_{RL,d} = \begin{pmatrix} 0 & 0 & ** \\ 0 & 0 & 0 \\ 0 & 0 & 0 \\ \vdots & \vdots & \vdots \end{pmatrix}, \qquad (11)$$

and $S_{RL,d}$ has the same form.

We can now use this notation to find out how sparse are the self-energy matrices. Using Eqs. (10) and (11) in the self-energy definitions of Eq. (7) we get

$$\Sigma_L^r(\epsilon) = (\epsilon S_{d,LL} - V_{d,LL}) G_L^{r0}(\epsilon)(\epsilon S_{LL,d} - V_{LL,d})$$

$$\sim \begin{pmatrix} ** & 0 & 0 & \cdots \\ 0 & 0 & 0 & \cdots \\ 0 & 0 & 0 & \cdots \end{pmatrix} \begin{pmatrix} ** & ** & \cdots \\ ** & ** & \cdots \\ \vdots & \vdots & \ddots \end{pmatrix} \begin{pmatrix} ** & 0 & 0 \\ 0 & 0 & 0 \\ 0 & 0 & 0 \\ \vdots & \vdots & \vdots \end{pmatrix}$$

$$= \begin{pmatrix} \sigma_L^r(\epsilon) & 0 & 0 \\ 0 & 0 & 0 \\ 0 & 0 & 0 \end{pmatrix}. \qquad (12)$$

The full square matrix at the second line of Eq. (12) stands for the isolated left lead rGF. As can be seen, the self-energy of the left lead can be represented by a very sparse matrix with only a single nonzero block, which we denote by σ_L^r.

A similar argument can be made for the self-energy of the right lead to get

$$\Sigma_R^r(\epsilon) = (\epsilon S_{d,\mathrm{RL}} - V_{d,\mathrm{RL}})G_R^{r0}(\epsilon)(\epsilon S_{\mathrm{RL},d} - V_{\mathrm{RL},d})$$

$$\sim \begin{pmatrix} 0 & 0 & 0 & \cdots \\ 0 & 0 & 0 & \cdots \\ ** & 0 & 0 & \cdots \end{pmatrix} \begin{pmatrix} ** & ** & \cdots \\ ** & ** & \cdots \\ \vdots & \vdots & \ddots \end{pmatrix} \begin{pmatrix} 0 & 0 & ** \\ 0 & 0 & 0 \\ 0 & 0 & 0 \\ \vdots & \vdots & \vdots \end{pmatrix}$$

$$= \begin{pmatrix} 0 & 0 & 0 \\ 0 & 0 & 0 \\ 0 & 0 & \sigma_R^r(\epsilon) \end{pmatrix}, \tag{13}$$

σ_R^r being the only nonzero block of Σ_R^r. Using Eqs. (8), (12), and (13) we find that the broadening matrices are also sparse,

$$\Gamma_L(\epsilon) = i[\Sigma_L^r(\epsilon) - \Sigma_L^a(\epsilon)] = \begin{pmatrix} \gamma_L(\epsilon) & 0 & 0 \\ 0 & 0 & 0 \\ 0 & 0 & 0 \end{pmatrix}, \tag{14}$$

and

$$\Gamma_R(\epsilon) = i[\Sigma_R^r(\epsilon) - \Sigma_R^a(\epsilon)] = \begin{pmatrix} 0 & 0 & 0 \\ 0 & 0 & 0 \\ 0 & 0 & \gamma_R(\epsilon) \end{pmatrix}, \tag{15}$$

where $\gamma_L = i(\sigma_L^r - \sigma_L^{r\dagger})$ and $\gamma_R = i(\sigma_R^r - \sigma_R^{r\dagger})$ stand for the nonzero blocks of the broadening matrices. Using the results of Eqs. (14) and (15) we can express the transmittance formula of Eq. (3) as follows (as before asterisks, circles, and boxes stand for nonzero blocks):

$$T(\epsilon) = \mathrm{Tr}[\Gamma_L(\epsilon)G_d^r(\epsilon)\Gamma_R(\epsilon)G_d^a(\epsilon)] \sim \mathrm{Tr}\left[\begin{pmatrix} \gamma_L & 0 & 0 \\ 0 & 0 & 0 \\ 0 & 0 & 0 \end{pmatrix}\right.$$

$$\times \begin{pmatrix} ** & ** & \bigcirc \\ ** & ** & ** \\ ** & ** & ** \end{pmatrix} \begin{pmatrix} 0 & 0 & 0 \\ 0 & 0 & 0 \\ 0 & 0 & \gamma_R \end{pmatrix} \begin{pmatrix} ** & ** & ** \\ ** & ** & ** \\ \bigcirc^\dagger & ** & ** \end{pmatrix}\right]$$

$$\sim \mathrm{Tr}\begin{pmatrix} \square & ** & ** \\ 0 & 0 & 0 \\ 0 & 0 & 0 \end{pmatrix}. \tag{16}$$

From Eq. (16) it can be seen that only the upper left ($\square$) diagonal block of the traced matrix is needed to be evaluated. The only contribution to this block from the device rGF is the upper right ($\bigcirc$) block of $G_d^r(\epsilon)$ which couples the left and the right parts of the device. The contribution from $G_d^a(\epsilon)$ is just the Hermitian conjugate of this block.

Therefore, as mentioned in Ref. 30, only the GF block corresponding to the lead-device junction regions is needed to be calculated explicitly and the dimensionality of the calculation scales with the length of the regions *directly* coupled to the leads rather than with the size of the full device. In this manner, very long devices can be treated efficiently.
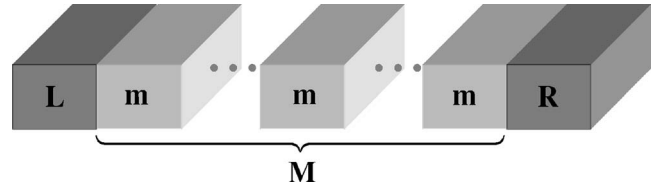

FIG. 2. A schematic representation of the subdivision of the device into the left (L), the middle (M), and the right (R) parts. The middle part is constructed by a replication of a repeating unit (m).

C. Green's function of a block tridiagonal Hamiltonian

We now turn to describe the calculation of the relevant blocks of the rGF of the device. We are interested in the calculation of the conductance through a very long system that has two end units and a middle part which is composed of a repeating unit cell. This setup is presented schematically in Fig. 2. We choose the end units and the middle part to be long enough such that we can approximately represent the finite replicated unit cell of the middle part by the corresponding part of an infinite periodic system.[50] We also choose this replicated unit cell to be long enough such that only nearest neighboring blocks interact. The Hamiltonian matrix of the device in a localized basis representation is then given by a block-tridiagonal matrix,[30,51,52]

$$H_d = \begin{pmatrix} H_L & H_{L,m} & & & & & & 0 \\ H_{L,m}^\dagger & H_m & H_{m,m} & & & & & \\ & H_{m,m}^\dagger & H_m & H_{m,m} & & & & \\ & & \ddots & \ddots & \ddots & & & \\ & & & H_{m,m}^\dagger & H_m & H_{m,m} & & \\ & & & & H_{m,m}^\dagger & H_m & H_{m,R} & \\ 0 & & & & & H_{m,R}^\dagger & H_R \end{pmatrix}. \tag{17}$$

Here, as before H_L (H_R) is the left (right) part Hamiltonian matrix, H_m is the repeating unit, m, Hamiltonian matrix, $H_{L,m}$ is the coupling matrix between the left part and the leftmost repeating unit, m, $H_{m,m}$ is the coupling between two adjacent repeating units of type m, and $H_{m,R}$ is the coupling matrix between the rightmost repeating unit m and the right part of the device. By approximating H_m as the corresponding infinite device real-space block matrix, we circumvent the problem of calculating the electronic structure of the full extended device ($L+M+R$) and replace it by the calculation of the considerably smaller $L+m+R$ setup. A similar representation, involving no approximations, can be written for the overlap matrix S_d.

Therefore, the device GF is given by the inverse of the block tridiagonal matrix $\epsilon S_d - H_D$. As described above, only a single block of the whole rGF of the device is needed for the conductance calculation. To evaluate this block we utilize an efficient scheme[53] that allows for the calculation of specific

submatrices of the inverse of a finite block tridiagonal matrix. Within this method the diagonal GF blocks of the device are given by

$$G_d^r(i,i) = [M_{i,i} - X_i - Y_i]^{-1},$$ (18)

where

$$X_{N-1} = 0,$$

$$X_{N-i} = M_{N-i,N-i+1}[M_{N-i+1,N-i+1} - X_{N-i+1}]^{-1}M_{N-i,N-i+1}^\dagger \quad 2 \leq i \leq N,$$ (20)

and Y_i is given by

$$Y_0 = 0,$$

$$Y_{i+1} = M_{i,i+1}^\dagger[M_{i,i} - Y_i]^{-1}M_{i,i+1}, \quad 0 \leq i \leq N-2,$$ (21)

where

$$M_{i,i+1} = \begin{cases} \epsilon S_{L,m} - H_{L,m}, & i = 0 \\ \epsilon S_{m,m} - H_{m,m}, & 0 < n < N-2 \\ \epsilon S_{m,R} - H_{m,R}, & i = N-2. \end{cases}$$ (22)

The off-diagonal blocks of the GF are given in terms of the corresponding diagonal blocks in the following manner:

$$G_d^r(i,j) = \begin{cases} C_i G_d^r(i-1,j), & i > j \\ D_i G_d^r(i+1,j), & i < j, \end{cases}$$ (23)

for $0 \leq i, j \leq N-1$ and the C_i and D_i coefficients are calculated by

$$C_i = -[M_{i,i} - X_i]^{-1}M_{i-1,i}^\dagger \quad 1 \leq i \leq N-1,$$

$$D_i = -[M_{i,i} - Y_i]^{-1}M_{i,i+1} \quad 0 \leq i \leq N-2.$$ (24)

Since we are only interested in the block that couples the left and right parts of the device, we are able to calculate this specific block while avoiding the calculation of the full (very large) GF of the device. To do this we first use Eq. (21) to calculate and store the Y_i matrices. Next, we calculate the last diagonal block of the GF, namely, $G_d^r(N-1,N-1)$, through Eq. (18). We finally obtain the required $G_d^r(0,N-1)$ block by calculating, in a recursive manner, X_n [Eq. (20)], D_n [Eq. (24)], and $G_d^r(n,N-1)$ [Eq. (23)] for $n = N-2,\ldots,0$.

For a density of states calculation we need the trace of the isolated rGF of the device multiplied by the overlap matrix,

$$\rho(E) = -\frac{1}{\pi} \text{Im}[\text{Tr}(G_d^{r0}S_d)];$$ (25)

therefore, all the information needed is contained in the diagonal and the first two off-diagonal blocks. These can be easily calculated using the procedure described above.

$$M_{i,i} = \begin{cases} \epsilon S_L - H_L - \sigma_L^r, & i = 0 \\ \epsilon S_m - H_m, & 0 < n < N-1 \\ \epsilon S_R - H_R - \sigma_R^r, & i = N-1. \end{cases}$$ (19)

Here, N is the number of blocks on the diagonal of the full matrix to be inverted. X_i is given by the following recursion relation:

D. Hamiltonian and overlap submatrice calculation

To obtain all the relevant submatrices needed for the conductance calculation we employ density functional theory (DFT). Molecular and periodic boundary condition (PBC) DFT calculations were carried out using the GAUSSIAN suite of programs.[54,55] Molecular orbitals (or Bloch functions in the PBC case) are expanded in terms of atomic Gaussian-type orbitals, and the Kohn-Sham (KS) equations are solved self-consistently in that basis set. The use of localized Gaussian-type orbitals as basis functions allows us to employ the formalism presented above.

The implementation of the conductance calculation is performed in six stages as described below.

(1) A one-dimensional PBC calculation for the left lead is performed. We extract the real-space KS and overlap matrices of the unit cell of the semi-infinite lead, as well as the KS and overlap coupling matrices between two adjacent unit cells within the lead. These matrices are then used to produce the rGF of the isolated semi-infinite left lead.[39–41]

(2) Same as the first stage but executed for the right lead. This stage can be skipped if the leads are identical.

(3) A one-dimensional PBC calculation for the repeating unit, m, is performed. We extract the real space KS matrices H_m and $H_{m,m}$ and the corresponding overlap matrices.

(4) In this stage we perform a molecular calculation for the isolated device ($L+m+R$ parts). We extract the following KS matrices: H_L, H_R, $H_{L,m}$, and $H_{m,R}$, and the corresponding overlap matrices.

(5) The goal of this stage is to calculate the KS and overlap coupling matrices between the left lead and the left part of the device. For that purpose we perform a one-dimensional PBC calculation of the left lead and the device ($LL+L+m+R$). The periodic direction is perpendicular to the elongated dimension of the device as shown in Fig. 1, and the unit cell of the left lead is chosen to be big enough such that the direct coupling between the elongated molecule and its replicated PBC images can be neglected. The extracted coupling matri-
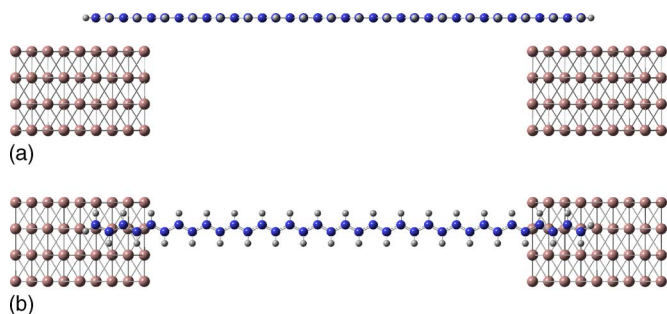
FIG. 3. Schematic side view (a) and top view (b) of the Al-TPA-Al junction employed for the transmittance calculations.

ces are the nonzero blocks represented by asterisks in Eq. (10).

(6)   Same as stage five, but executed for the right lead.

The output submatrices of each one of these six stages are stored in separate files. These matrices are then employed to calculate the conductance using the method described in the previous sections.

III. PROOF OF CONCEPT

In order to evaluate the proposed method, we calculate the transmittance probability through a TPA chain coupled to two aluminum leads (see Fig. 3). This simple model system allows us to systematically compare the results of our approach to those of a full scale calculation. We choose a setup in which TPA physisorbs on top of the leads similar to the setup commonly used in elongated system conductance measurements.[12,26] The lead replicated unit cells are represented by two fcc slabs comprising of 72 aluminum atoms each with a lattice constant of 4.05 Å. The total length of the TPA chain is 18 unit cells, where each unit cell contains two carbon-hydrogen pairs. The TPA geometry was taken from Ref. 56. We divide the TPA chain such that the left, middle, and right parts of it consist of six unit cells each. The distance between the TPA chain and the aluminum surface is fixed at ~3 Å.

Since we are interested in proof of concept, we use a minimal STO-3G basis set within the local density approximation (RSVWN5 keyword in GAUSSIAN) for both the leads and the TPA chain. This enables us to readily perform the full scale calculation for the elongated device and compare the results to those obtained by the divide and conquer approach.

In Fig. 4 we present the transmittance probability through a 30 unit cell length TPA chain at an energy window of 1 eV around the Fermi energy of the leads. We compare the result obtained using our divide and conquer approach (solid black line in the figure) to those obtained for the full 30 unit cell TPA chain (dashed red line). For the divide and conquer calculation we use a $6-6\times3-6$ TPA chain where the notation $A-B\times n-C$ stands for a left part comprising of A unit cells, a middle part comprising of B unit cells replicated n times, and a right part comprising of C unit cells.

As can be seen in Fig. 4, the divide and conquer calculation is able to correctly capture the physical features obtained by the full transmittance calculation in the energy re-
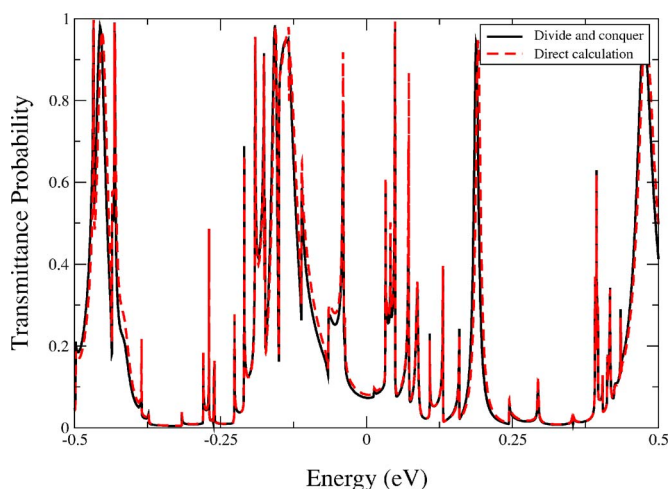

FIG. 4. The transmittance probability through a 30 unit cell long TPA chain. The solid black line is the divide and conquer approach calculation for a $6-6\times3-6$ TPA system. The dashed red line is a direct calculation for the full length TPA chain. The Fermi energy of the leads (2.00 eV) is set to 0. In this scale, the Fermi energy of the infinite periodic TPA chain is −3.66 eV.

gion explored. The source for the minor differences between the two curves can be traced back to two approximations done during the calculation. The first approximation is the truncation of the Hamiltonian and overlap matrices when dividing the device into the different blocks. This approximation can be systematically improved by increasing the size of the blocks. The second (and more subtle) approximation is the fact that we represent all the m blocks (see Fig. 2) by the real-space block of the corresponding infinite periodic system. For a full scale self-consistent calculation this, of course, is not correct and an m block adjacent to the left (or right) part of the molecule will have a somewhat different Hamiltonian matrix than a corresponding block near the middle of the elongated system. This approximation can be relived by including some of the middle part repeating units in the left and right parts of the molecule.

Despite the approximations mentioned above, the correspondence between the curves is remarkable. There does not seem to exist a constant shift between the curves, as one may expect due to the difference in the Fermi energies between the finite TPA chain and the infinite periodic TPA system used to produce the divide and conquer results. Such a shift is not observed due to the fact that for the finite (30 unit cells long) system considered, the Fermi energy is calculated to be very close to that of the infinite system.

A similar analysis has been performed for the transmittance probability in the vicinity of the Fermi energy of the TPA chain. As can be seen in Fig. 5, the divide and conquer method produces a very good transmittance probability estimation for a region of 0.8 eV around the Fermi energy of the infinite periodic TPA system. The general location of the regions of high transmittance around ±0.45 eV is also captured well, although some peaks appear to be shifted and altered (shown as an inset in Fig. 5).

At this point it is worth mentioning that there is no direct measure of the accuracy of the divide and conquer method with respect to the full scale calculation. Nevertheless, a systematic route to investigate how well the method captures the
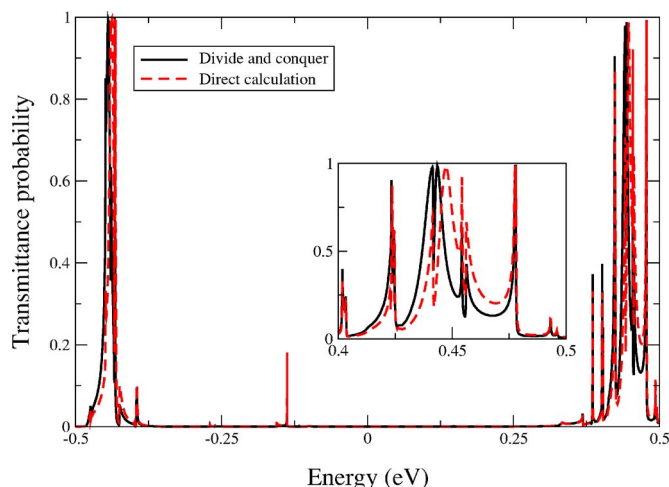
FIG. 5. The transmittance probability through a 30 unit cell long TPA chain. The solid black line is the divide and conquer approach calculation for a $6-6 \times 3-6$ TPA system. The dashed red line is a direct calculation for the full length TPA chain. The Fermi energy of the infinite periodic TPA chain (-1.66 eV) is set to 0. In this scale, the Fermi energy of the leads is 3.66 eV. Inset: zoom in on the region of 0.4–0.5 eV.
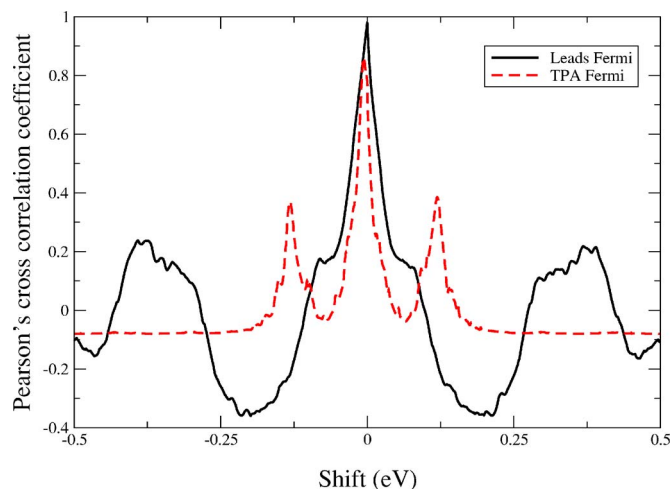

FIG. 6. The cross-correlation coefficient comparing the direct transmittance probability calculation with the divide and conquer method for the energy region around the Fermi energy of the leads (solid black curve) and around the Fermi energy of an infinite periodic TPA chain (dashed red curve).

direct calculation results would be to check the sensitivity of the calculated transmittance probability to an increase (or decrease) of the size of the elongated device blocks.

In order to quantify our results we apply a linear cross-correlation analysis utilizing Pearson's formula.[57] Given two discrete data sets X_i and Y_i, where $0 \leqslant i \leqslant M$ one can calculate their cross-correlation using the following formula:

$$r(d) = \frac{\Sigma_i [(X_i - \bar{X})(Y_{i-d} - \bar{Y})]}{\sqrt{\Sigma_i (X_i - \bar{X})^2} \sqrt{\Sigma_i (Y_{i-d} - \bar{Y})^2}}. \qquad (26)$$

Here r is the cross-correlation factor, $\bar{X}$ is the mean value of the X_i data set, $\bar{Y}$ is the mean value of the Y_i data set, and d is a shift we apply to the Y_i data set. For each shift we calculate the cross-correlation coefficient, r. We assume circular symmetry of the data sets such that whenever the index deviates from the data set boundaries it is folded back into the allowed region. The cross-correlation factor of Eq. (26) is normalized such that $-1 \leqslant r \leqslant 1$. When $r=1$ the two sets are completely correlated, when $r=-1$ one set is completely correlated with the inverse of the other set, and when $r=0$ there is no significant correlation between the two sets.

In Fig. 6 we present the cross correlation of the transmittance probability curves obtained by the divide and conquer approach and by the direct calculation, for both energy regions studied. As can be seen from the solid black curve, the two calculations around the Fermi energy of the leads are highly correlated ($r=0.98$) at zero shift. This verifies our previous qualitative findings that all the physical features arising from the full device calculation are captured by the divide and conquer approach at this energy region and that there is no constant shift between the two diagrams. As expected from the analysis of Fig. 5, the peak correlation for the energy region around the Fermi energy of the TPA periodic system is slightly shifted to the negative shift region, and has a somewhat lower (yet still significant) value of $r = 0.86$.

IV. SUMMARY

In this paper we present a method to evaluate the transmittance probability and the coherent conductance through elongated molecules composed of a repeating unit and terminated at both ends. The method is based on a divide and conquer approach in which the Hamiltonian matrix of the elongated molecule in a localized basis set representation can be regarded as a block tridiagonal matrix. By approximating the Hamiltonian matrix blocks of the middle part of the elongated molecule by those of the corresponding infinite periodic system, we circumvent electronic structure calculations involving the entire open system. Employing dimensionality scaling arguments relevant to the calculation of the conductance through such systems, we have been able to efficiently obtain the GF submatrices needed for the evaluation of the transmittance probability.

Using our approach, computational efforts can be reduced in both the electronic structure part of the calculation and the GF conductance evaluation. This allows us to evaluate the transmittance probability and the conductance of a one-dimensional finite sized extended system using first-principles electronic structure methods. To this end we have employed density functional theory in the Kohn-Sham framework and Gaussian basis functions.

A proof of concept model based on a *trans*-polyacetylene chain bridging two aluminum leads indicates that our divide and conquer approach is able to capture all the physical features appearing in the transmittance probability curves of a full scale calculation. Work in the direction of calculating the conductance through extended systems such as carbon nanotubes, graphene ribbons, and DNA is currently under progress. It is worth mentioning that our method is not restricted to the simplified Landauer picture presented in the current study. Extensions to nonequilibrium Green's function calculations or absorbing potential treatments should be relatively straight forward.

In recent studies, the ground state electronic structure of elongated systems was accurately captured[58,59] using hybrid

functionals, such as the screened exchange hybrid functional of Heyd, Scuseria, and Ernzerhof[60] (HSE) within the framework of DFT. The combination of the current method with the utilization of such state of the art electronic structure calculations including electron-electron interaction effects may lead to a better understanding of the electronic transport properties through elongated systems.

ACKNOWLEDGMENTS

[1] A. Aviram and M. A. Ratner, Chem. Phys. Lett. **29**, 277 (1974).
[2] J. Jortner and M. Ratner, *Molecular Electronics* (Blackwell Science Inc., New York, 1997).
[3] C. Roth and C. Joachim, *Atomic and Molecular Wires* (Kluwer, Dordrecht, 1997).
[4] E. G. Emberly and G. Kirczenow, Ann. N.Y. Acad. Sci. **852**, 54 (1998).
[5] M. Ratner, Nature (London) **404**, 137 (2000).
[6] C. Joachim, J. K. Gimzewski, and A. Aviram, Nature (London) **408**, 541 (2000).
[7] J. M. Tour, Acc. Chem. Res. **33**, 791 (2000).
[8] A. Nitzan, Annu. Rev. Phys. Chem. **52**, 681 (2001).
[9] S. T. Pantelides, M. D. Ventra, and N. D. Lang, Physica B **296**, 72 (2001).
[10] A. Nitzan and M. A. Ratner, Science **300**, 1384 (2003).
[11] J. R. Heath and M. A. Ratner, Phys. Today **56**(5), 43 (2003).
[12] S. J. Tans, M. H. Devoret, H. Dai, A. Thess, R. E. Smalley, L. J. Geerligs, and C. Dekker, Nature (London) **386**, 474 (1997).
[13] S. J. Tans, A. R. M. Verschueren, and C. Dekker, Nature (London) **393**, 49 (1998).
[14] Z. Yao, H. W. C. Postma, L. Balents, and C. Dekker, Nature (London) **402**, 273 (1999).
[15] C. Dekker, Phys. Today **52**(5), 22 (1999).
[16] A. Bachtold, P. Hadley, T. Nakanishi, and C. Dekker, Science **294**, 1317 (2001).
[17] W. Liang, M. Bockrath, D. Bozovic, J. H. Hafner, M. Tinkham, and H. Park, Nature (London) **411**, 665 (2001).
[18] P. Avouris, Acc. Chem. Res. **35**, 1026 (2002).
[19] O. Hod, E. Rabani, and R. Baer, J. Chem. Phys. **123**, 051103 (2005).
[20] O. Hod, E. Rabani, and R. Baer, Acc. Chem. Res. **39**, 109 (2006).
[21] K. S. Novoselov, A. K. Geim, S. V. Morozov, D. Jiang, Y. Zhang, S. V. Dubonos, I. V. Grigorieva, and A. A. Firsov, Science **306**, 666 (2004).
[22] C. Berger, Z. Song, X. Li, X. Wu, N. Brown, C. Naud, D. Mayou, T. Li, J. Hass, A. N. Marchenkov, E. H. Contrad, P. N. First, and W. A. de Heer, Science **312**, 1191 (2006).
[23] J. C. Scott, Science **278**, 2071 (1997).
[24] R. Friend, Nature (London) **441**, 37 (2006).
[25] K. Lee, S. Cho, S. H. Park, A. J. Heeger, C.-W. Lee, and S.-H. Lee, Nature (London) **441**, 65 (2006).
[26] D. Porath, A. Bezryadin, S. de Vries, and C. Dekker, Nature (London) **403**, 635 (2000).
[27] P. J. de Pablo, F. Moreno-Herrero, J. Colchero, J. G. Herrero, P. Herrero, A. M. Baró, P. Ordejón, J. M. Soler, and E. Artacho, Phys. Rev. Lett. **85**, 4992 (2000).
[28] A. Y. Kasumov, M. Kociak, S. Guéron, B. Reulet, V. T. Volkov, D. V. Klinov, and H. Bouchiat, Science **291**, 280 (2001).
[29] A. Rakitin, P. Aich, C. Papadopoulos, Y. Kobzar, A. S. Vedeneev, J. S. Lee, and J. M. Xu, Phys. Rev. Lett. **86**, 3670 (2001).
[30] M. P. Anantram and T. R. Govindan, Phys. Rev. B **58**, 4882 (1998).
[31] D. Orlikowski, H. Mehrez, J. Taylor, H. Guo, J. Wang, and C. Roland, Phys. Rev. B **63**, 155412 (2001).
[32] S. Krompiewski, J. Martinek, and J. Barnaś, Phys. Rev. B **66**, 073412 (2002).
[33] S. Compernolle, L. Chibotaru, and A. Ceulemans, J. Chem. Phys. **119**, 2854 (2003).
[34] A. N. Andriotis, M. Menon, and L. Chernozatonskii, Nano Lett. **3**, 131 (2003).
[35] Y. Xue and M. A. Ratner, Phys. Rev. B **70**, 205416 (2004).
[36] W. Zhang, W. Lu, and E. G. Wang, Phys. Rev. B **72**, 075438 (2005).
[37] M. B. Nardelli, J.-L. Fattebert, and J. Bernholc, Phys. Rev. B **64**, 245423 (2001).
[38] D. H. Lee and J. D. Joannopoulos, Phys. Rev. B **23**, 4997 (1981).
[39] M. P. López-Sancho, J. M. López-Sancho, and J. Rubio, J. Phys. F: Met. Phys. **14**, 1205 (1984).
[40] M. P. López-Sancho, J. M. López-Sancho, and J. Rubio, J. Phys. F: Met. Phys. **15**, 851 (1985).
[41] M. B. Nardelli, Phys. Rev. B **60**, 7828 (1999).
[42] M. B. Nardelli and J. Bernholc, Phys. Rev. B **60**, R16338 (1999).
[43] W. Lu, V. Meunier, and J. Bernholc, Phys. Rev. Lett. **95**, 206805 (2005).
[44] R. Landauer, IBM J. Res. Dev. **1**, 223 (1957).
[45] R. Landauer, Philos. Mag. **21**, 836 (1970).
[46] S. Datta, *Electronic Transport in Mesoscopic Systems* (Cambridge University Press, Cambridge, 1995).
[47] A. Nitzan, M. Galperin, G. Ingold, and H. Grabert, J. Chem. Phys. **117**, 10837 (2002).
[48] T. N. Todorov, G. A. D. Briggs, and A. P. Sutton, J. Phys.: Condens. Matter **5**, 2389 (1993).
[49] M. Paulsson, e-print cond-mat/0210519.
[50] J. Jiang, W. Lu, and Y. Luo, Chem. Phys. Lett. **416**, 272 (2005).
[51] J. Taylor, H. Guo, and J. Wang, Phys. Rev. B **63**, 245407 (2001).
[52] A. Schnurpfeil and M. Albrecht, Theor. Chem. Acc. (to be published).
[53] E. M. Godfrin, J. Phys.: Condens. Matter **3**, 7843 (1991).
[54] M. J. Frisch, G. W. Trucks, H. B. Schlege *et al.*, GAUSSIAN *Development Version*, Revision C.01, Gaussian, Inc., Wallingford, CT, 2004.
[55] K. N. Kudin and G. E. Scuseria, Phys. Rev. B **61**, 16440 (2000).
[56] R. Pino and G. E. Scuseria, J. Chem. Phys. **121**, 8113 (2004).
[57] W. H. Press, S. A. Teukolsky, W. T. Vetterling, and B. P. Flannery, *Numerical Recipes in C++: The Art of Scientific Computing* (Cambridge University Press, Cambridge, 2002).
[58] V. Barone, J. E. Peralta, M. Wert, J. Heyd, and G. E. Scuseria, Nano Lett. **5**, 1621 (2005).
[59] V. Barone, J. E. Peralta, and G. E. Scuseria, Nano Lett. **5**, 1830 (2005).
[60] J. Heyd, G. E. Scuseria, and M. Ernzerhof, J. Chem. Phys. **118**, 8207 (2003); **124**, 219906(E) (2006).